International Journal of Medical and Health Sciences Research
ISSN(e): 2313-2752/ISSN(p): 2313-7746

URL: www.pakinsight.com

MODEL FOR ABSORPTION OF PERFLUOROPROPANE INTRAOCULAR GAS AFTER RETINAL SURGERIES

A. Terry Bahill[1]
[1]*Systems and Biomedical Engineering University of Arizona*

ABSTRACT

Purpose: The intended audience for this paper is retina surgeons who perform retinal detachment (RD) operations, anesthesiologists and dentists who use nitrous oxide, ophthalmologists and optometrists who encounter RD patients, students of ophthalmology and optometry, and RD patients, their families and friends. To help future retinal detachment (RD) and macular hole patients understand imminent eerie visual events, the author developed a mathematical model for the behavior of an injected intraocular C_3F_8 perfluoropropane gas bubble after an RD operation. Ophthalmologists could use this model to create animations showing patients what to expect. Methods: Our subject had three RD operations with the injection of perfluoropropane gas. After each of these operations, he daily recorded the horizon to gas bubble angle and the radius of curvature of the gas bubble. These data were used to calculate the volume and surface area of the gas bubble. Then formal modeling techniques were applied. Results:One gas bubble, which lasted 73 days, was studied extensively. Fitting the measured data required four geometric submodels, corresponding to the four possible bubble configurations. Conclusions: This model for the absorption of an intraocular gas bubble had two components: the structural component described the four geometric configurations that the bubble went through in its lifecycle and the dynamic component that described the absorption rate of the gas. The model suggests that the gas-bubble absorption-rate is not proportional to either the surface area of the bubble or the surface area between the SF6 gas and the aqueous humour. Rather the gas-bubble absorption-rate is proportional to the surface area of gas in contact with the retina.

Keywords: Complications, Modeling, Perfluoropropane gas bubble, Rate of absorption, Retinal detachment surgery.

Received: 28 March 2016/ **Revised:** 18 June 2016/ **Accepted:** 24 August 2016/ **Published:** 19 September 2016

Contribution/ Originality

This is the first paper to show the four sequential geometric models of an intraocular perfluoropropane gas bubble after a retinal detachment operation. This bubble is absorbed at a rate proportional to the amount of gas in direct contact with the retinal surface.

1. INTRODUCTION

Our subject, A. Terry Bahill, had a dozen eye surgeries in a five-year period [1]. He was examined and treated by an optometrist and ten ophthalmologists. This paper describes a small subset of his experiences. This section was written from the subject's point of view, therefore, it was written in the first person singular.

DOI: 10.18488/journal.9/2016.3.5/9.5.50.76
ISSN(e): 2313-2752/ISSN(p): 2313-7746

On May 12, 2008, my optometrist saw a half-dozen retinal tears (like tears in a fabric, not like tears when a person is crying) and referred me to a retina specialist. He suggested operating that evening. He told me that the operation had a 92% probability of success and if it failed, he could do another operation that had a 50% probability of success. During that first retinal operation, he removed the vitreous, installed a scleral buckle and injected a bubble of perfluoropropane (C_3F_8) gas (also called octafluoropropane). He told my wife and me to be patient for six weeks, or until the gas bubble disappeared, then we would be out of the woods for further complications.

Therefore, after 49 days, we were in high spirits because the gas bubble was completely absorbed. However, he examined my eye and suggested another retinal detachment operation. On July 1, he injected another gas bubble. That second bubble, which lasted 73 days, is the subject of this paper.

An intraocular gas bubble prevents liquid from contacting the retinal tear and sneaking under the retina. This barrier allows the choroid to remove subretinal fluid and shelters the tear until a choroid-retinal scar is formed, sealing the break. Also, if the subject's head is held in a certain position, the buoyancy of the bubble will help hold the retina against the choroid. A bubble of perfluoropropane (C_3F_8) gas will gradually be absorbed into the blood stream and will be replaced by aqueous humor liquid, which is continually produced by the ciliary body. This process takes from three to eleven weeks, depending on the type, amount of gas, concentration of the gas, use of eye drops, intraocular pressure and other physiological characteristics of the individual.

In September, my ophthalmologist found a new tear in my retina. He repaired it with 60 pulses of a head mounted laser. He inserted a cryopexy probe on top of the eyeball near the scleral buckle to freeze (cryopexy) the area of the retina above the tear. He removed some fluid from the eyeball and injected another bubble of C_3F_8. The next day he administered 567 laser pulses. This third bubble was smaller than the other two and remained only 20 days.

The lifetimes of the gas bubbles (49, 73 and 20 days) are only important for showing the variability that can be expected. The first and second operations had the same patient, eye, year, hospital, surgeon, technique, laser photocoagulation, eye drops, amount of C_3F_8 gas and post-operation head position instructions. However, their gas bubble durations were different. From this, we conclude that a patient would not be able to predict the lifetime of a bubble. Although the lifetimes of the three bubbles were different, the shapes of the radius of curvature data were similar for the three operations.

The following comments may be irrelevant. A year before the first RD, I had an abnormal cataract extraction. The posterior membrane capsule ruptured during the surgery, so the lens was placed in the ciliary sulcus. Four years later a subsequent ophthalmologist noted, "The left pupil was 3×4 mm, oval, and peaked at the 11 o'clock position… posterior synechiae at the superonasal optic-haptic junction…. The iris is stuck to the optic-haptic junction at this location." The pupil has been unresponsive for eight years now. I was always myopic and in the first RD surgery a scleral buckle was installed: these details affect the size of the eyeball. The first RD was six tears from 5 o'clock to 8 o'clock. The second was a superior-temporal tear at 1 o'clock and the third RD was a single break at 12 o'clock. After the second operation and for the next five years I also had cystoid macular edema. In an effort to relieve this edema, in a fourth operation the surgeon peeled off the inner limiting membrane (ILM). This did not help the edema but it did leave me colour blind in the fovea of the left eye [2].

We developed a model to help understand the absorption of an intraocular C_3F_8 gas bubble. This model has two components, structure and dynamics. The first describes the four geometric configurations that the bubble seems to go through in its lifecycle and the second describes the rate of absorption of a gas bubble.

2. MATERIALS AND METHODS

2.1. Modeling Methods

A *model* is a simplified representation of some aspect of a real system. A *simulation* is an implementation of a model, often on a digital computer. Models are ephemeral: they are created, they explain a phenomenon, they

stimulate discussion, they foment alternatives and then they are replaced by new models [3]. Everyone knows how to make a model, but most researchers miss a few steps. Therefore, we wrote this section that presents a succinct description of the modeling process.

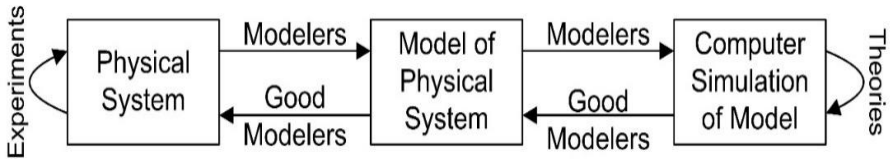

Fig-1. Modeling philosophy

2.1.1. Tasks in the Modeling Process

The following checklist contains the principle tasks that should be performed in a modeling study. The modelers should look at each item on the list and ask if they have done that task. If not, they should state why they did not do it. In this checklist, we describe {in curly braces} the parts of this gas bubble absorption model that satisfy the individual tasks.

- Describe the system to be modeled {The absorption of an intraocular perfluoropropane gas bubble injected during a retinal detachment operation.}
- State the purpose of the model {To help retinal detachment (RD) patients understand forthcoming peculiar visual events.}
- Determine the level of the model {This model concerns the size and shape of the gas bubble and the eyeball, thus units of centimeters (cm) are appropriate. The time scale is in days.}
- State the assumptions and at every review reassess the assumptions. This is a hard, but important task. {① Humans are basically alike. ② Absorption of intraocular gas is a continuous process and daily sampling is sufficient. ③ The human is capable of measuring the two optical parameters that are needed to characterize the system. ④ The diameter of the subject's eyeball is 2.2 cm. ⑤ "1 ml of pure C_3F_8 gas injected pars plana" would produce an intraocular bubble of 4 ml by day 4. ⑥ The gas bubble stayed in the vitreous cavity and did not enter the anterior chamber. ⑦ The volume of the vitreous cavity is 5 ml. At every review, we reassessed these assumptions and found them to be reasonable, although our subject is myopic.}
- Investigate alternative models, both original and from the literature {Rate of absorption is proportional to the volume, surface area and geometry of the gas bubble.}
- Select a tool or language for the model and simulation {We used Euclidean geometry and diffusion equations.}
- Make the model. Models are often arranged in hierarchies. {Our model had two components: the first described the four geometric configurations that a bubble goes through in its lifecycle and the second described the rate of absorption of the gas.}
- Integrate with models for other systems {The ciliary body must produce the aqueous humor liquid and the choroid must take away C_3F_8 gas. Intraocular pressure must be monitored to forestall glaucoma. Visual acuity and diplopia must be measured and tracked.}
- Gather data describing system behavior {We used subject-recorded data from three retinal detachment operations.}
- Show that the model behaves like the real system {The figures of this paper show this.}
- Verify and validate the model {The model describes the absorption of intraocular C_3F_8 gas. This should help RD patients understand their strange visual environments.}

- Explain something not used in the model's design {①The model shows the points in time when the physiological system switched from one geometric configuration to another. ②The sketch of the big dipper fits into the subject's field of view (FoV).}
- Perform a sensitivity analysis {Our model's fit to the measured data was most sensitive when model-3 was manifest, when the bubble surface was meniscus shaped. These data have the least reliability, because the subject lacked the knowledge, experience and equipment to measure the radius of curvature accurately.}
- Use the model to perform a risk analysis {Our risk analysis explained why it would be dangerous for patients to fly in airplanes, scuba dive or have nitrous oxide anesthesia.}
- Analyze the performance of the model {To do this, we will need a new RD patient with an intraocular C_3F_8 gas bubble.}. This study begs for a repetition.
- Re-evaluate and improve the model {To do this we need a new patient who will collect intraocular gas data after a RD operation.}
- Design new experiments and measurements on the real system {New RD patients should be encouraged to collect similar data after their retinal detachment operations. Guided by this paper, they will be able to look for the bubble surface during the first few days. Ophthalmologists should record the amount of gas injected and their predictions of the bubble lifetime.}

2.1.2. Purpose of Models

Models can be used for many reasons, such as understanding or improving an existing system (this paper), creating a new design or system, controlling a system, suggesting new experiments (this paper), guiding data collection activities (this paper), allocating resources, identifying cost drivers, increasing return on investment, identifying bottlenecks, helping to sell the product, and reducing risk (this paper).

2.1.3. Different Types of Models

There are many types of models. Most people use only a few and think that is all there are. Here is a partial list of some of the most commonly used types of models: differential or difference equations, geometric representation of physical structure, computer simulations and animations, Laplace transforms, transfer functions, linear systems theory, state space models, e. g. $\dot{x} = \mathbf{A}x + \mathbf{B}u$, state machine diagrams, charts, graphs, drawings, pictures, functional flow block diagrams, object-oriented models, UML and SysML diagrams, Markov processes, time-series models, algebraic equations, physical analogs, Monte Carlo simulations, statistical distributions, mathematical programming, financial models, Pert charts, Gantt charts, risk analyses, tradeoff studies, mental models, scenarios and use cases.

Most models require a combination of these types. For example, our model for the absorption of intraocular gas had two components, structure and dynamics. For the structure, we used *charts*, *graphs*, *drawings* and *algebraic equations* to describe the four geometric configurations that a bubble goes through in its lifecycle. For the dynamics, we needed a *set of equations* that described the time-dependent behavior of the system. The absorption of intraocular gas has only one state, so we only needed one time-dependent *differential equation* to describe the *system state*. So our model used more than a half-dozen types of models.

2.1.4. Model-Based Design

There are two common techniques for designing systems: the first is model-based [4] and the second is databased. Here are some steps for model-based system design. Find appropriate physical and/or physiological principles, then using the tasks listed above, design, build and test a model, and design experiments to collect data. Use this data to verify and validate the model. Use the model to make predictions and guide future data collection activities.

Example 1

To model the absorption of an intraocular gas bubble, we could use the physical principle that the time rate of change of the volume of a gas bubble (also called the rate of absorption) is proportional to the volume: $\frac{dV}{dt} = -kV$ [5]; [6].

Nomenclature Note:

The following terms are equivalent: the rate of absorption of the gas, the absorption rate, the time rate of change of the gas volume, the derivative of the gas volume equation, and the slope of the gas volume curve. For volumes, the following units are identical: cubic centimeters (cm^3 and cc) and milliliters (ml and mL).

Example 2

[7] proposed a model for the absorption of a gas bubble in the eye where the rate of change of the gas volume was proportional to the amount of gas in direct contact with the retinal surface: $\frac{dV}{dt} = -k \times SA \times P_{ab} \times velocity$,

where *V* is the volume of the gas, *SA* is the area of the bubble in contact with the retina, P_{ab} is the probability of absorption of a molecule at the gas-retina interface and *velocity* is that of the molecules in the gas. He found that the biggest differences between his model and an exponential model occurred near the end of the absorption period, so that is where he focused most of his *data collection activities*.

2.1.5. Data-Based Design

The second technique for designing a system is databased. With this technique, the modeler starts with measuring and organizing the data and then he or she makes a model that fits that measured data. We used that technique in this study.

2.2. Method for Collecting Data

We modeled the eyeball as a sphere with an inside diameter of 2.2 cm. Therefore the volume of the eyeball is $V = \frac{4\pi}{3} R^3 = 5.6 \text{ ml}$. However, the gas bubble was injected into the vitreous cavity and it probably did not enter the anterior chamber. So when we subtracted the volume of the anterior chamber and the lens, we get a volume for the vitreous cavity of 5 ml. As a consistency check, we note that during vitreoretinal surgery, the surgeon typically uses 50 ml gas syringe. He uses 35 ml to flush the system (40 ml for myopic eyes) to leave 4 or 5 ml of gas in the eyeball [8]. Therefore, our 5 ml volume is consistent with the literature on retinal surgery. Furthermore, in the first and second operations on this subject, one ml of pure C_3F_8 gas was injected. This would have expanded to 4 ml by the fourth day. However, the eyeball volume is increased in myopic eyes and is decreased by scleral buckles. Our number is not exact: we did not measure the inside diameter of our subject's eyeball and he was myopic, pseudophakic and had a scleral buckle. Therefore for our model, a diameter of 2.2 cm and a volume of 5 ml are very good values.

To determine the rate of absorption of the C_3F_8 gas bubble, we needed the size and shape of the gas bubble. The inputs to our system were the two optical parameters that our subject measured: the horizon to bubble distance and the radius of curvature of the bubble.

Figure 2 shows a side-view (sagittal section) of the eye showing the *horizon to bubble distance* and its relationship to *offset* of the gas in the eyeball.

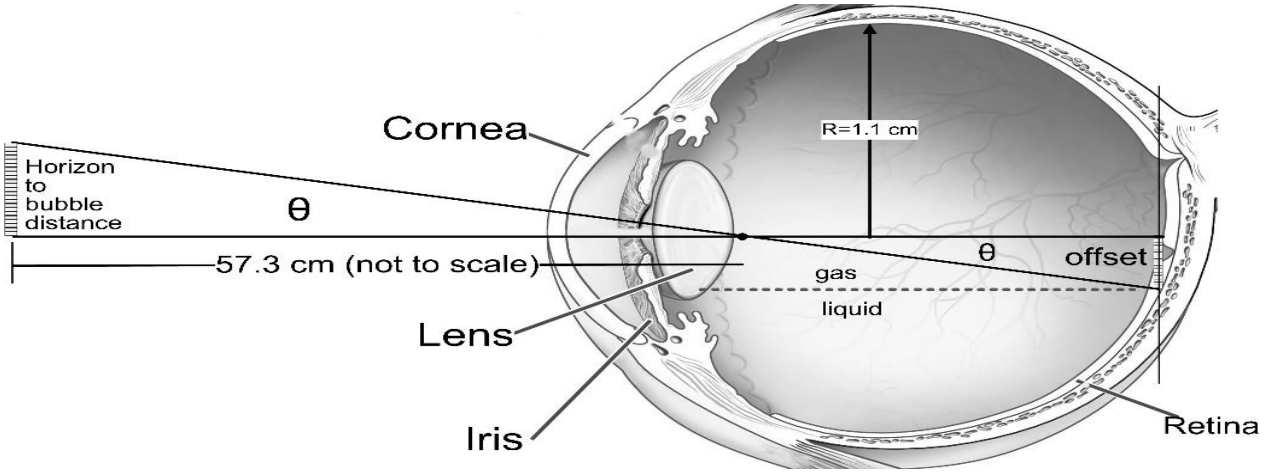

Fig-2. Side-view of the eye (sagittal section) showing the *horizon to bubble distance* and its relationship to the offset between the gas-liquid surface and the center of the eye. This drawing is not to scale (cm inside the eyeball are different from cm outside the eyeball)

A week or so after the gas injection, after some of the gas had been absorbed so that the subject could see part of the bubble's surface, the subject measured the *horizon to bubble distance*. To do this, he held a half-meter stick at arm's length, put the bottom of the stick on the horizon and measured the distance to the edge of the bubble's image. An observer carefully watched the subject to make sure that he was holding the meter stick at arm's length, 57.3 cm (23 inches) away from the eye. At this distance, one cm in space corresponds to one degree of visual angle.

2.2.1. Geometry of the Eyeball

In order to convert the measured horizon to bubble distance into the offset between the liquid-gas surface and the center of the eye, we need two factors, one that that relates the size of a physical object to the size of its image on the retina given the optics of the eye and a second that relates the size of the image on the retina to the offset between the gas-liquid surface and the center of the eye.

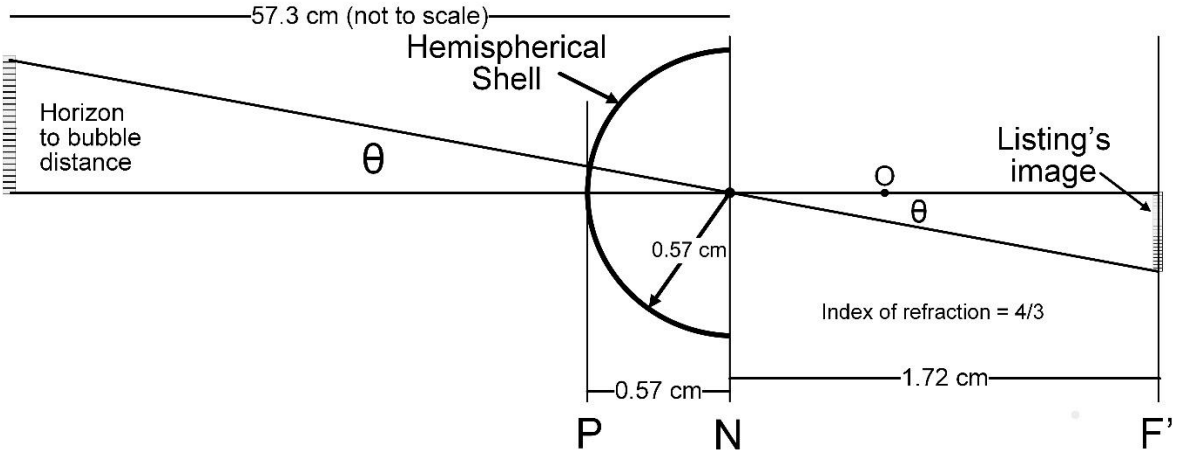

Fig-3. Listing's reduced eye model for the human. All of the eye's optical properties are modeled with a single hemispherical shell.

Figure 3 shows Listing's reduced human eye model. All of the eye's optical properties are modeled with a single hemispherical shell with its center 1.72 cm from the retina. All of the ocular media are modeled with a uniform index

of refraction of 4/3: this would be needed if we used Snell's law of refraction. This is a model, which means that it is a simplification of a real world system, for example the drawing is not to scale (cm inside the eyeball are different from cm outside the eyeball). For small angles

$$\frac{Horizon\ to\ bubble\ \text{distance}}{57.3} = \tan\theta = \frac{Listing's\ image}{1.72}$$

Therefore,

the size of *Listing's image* is $\frac{1.72}{57.3}$ times the *horizon to bubble distance*. This is a good approximation for small angles. However, with a little trigonometry and figure 4, we can get a better value for the offset between the liquid-gas surface and the center of the eye.

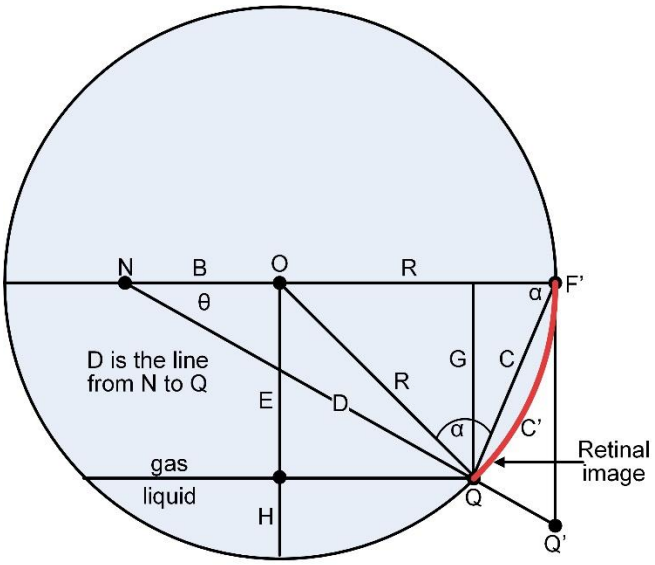

Fig-4. Geometric relationship between the retinal image and the offset between the gas-liquid surface and the center of the eye.

Listing's reduced eye model gives the size of an image on a plane tangent to the retina (labeled *C'*). But we really want the size of the image on the retina (the thick red arc in figure 4). We can approximate this with the chord of the circle, *C*, shown in figure 4. For large angles like 35° this gives an error of only one degree. Then, using the triangle OQF' we can write the length of the chord

$$C = 2R\cos\alpha$$

$$E = G = C\sin\alpha$$

$$\sin^2 x + \cos^2 x = 1$$

$$E = C\sqrt{1 - \frac{C^2}{4R^2}}$$

Thus, we have the offset (*E*) between the liquid-gas surface and the center of the eye in cm as a function of the retinal image size (approximated with *C*). Now we must combine the results of figures 3 and 4. The *retinal image*, *C*, is $\frac{1.72}{57.3}$ times the *horizon to bubble distance*. Therefore, in our spreadsheet we use $Offset = \frac{1.72}{57.3} C\sqrt{1 - \frac{C^2}{4R^2}}$

where *C* is the length of the chord approximating the retinal image size.

Similarly the *radius of curvature* of the bubble

$r = \frac{1}{2} \times \frac{1.72}{57.3} C \sqrt{1 - \frac{C^2}{4R^2}}$, where *C* is the diameter of the bubble's image.

We will now derive the offset (*E*) between the gas-liquid surface and the center of the eye as a function of the angle θ. We used this formula to verify calculations that we made using the above formulae. Let us start with the triangle ONQ, with *D* being the line from N to Q.

By the law of cosines

$$R^2 = B^2 + D^2 - 2BD\cos\theta$$

$$D^2 - 2BD\cos\theta + B^2 - R^2 = 0$$

Now we use the quadratic formula to solve for *D*.

$$D = \frac{2B\cos\theta \pm \sqrt{4B^2\cos^2\theta - 4\left(B^2 - R^2\right)}}{2}$$

$$D = B\cos\theta \pm \sqrt{B^2\cos^2\theta - \left(B^2 - R^2\right)}$$

Because $B < R$

$$D = B\cos\theta \pm \sqrt{B^2\cos^2\theta + \text{positive number}}$$

So one root is positive and the other is negative. We ignore the negative root and remove the minus sign in front of the radical sign.

$$D = B\cos\theta + \sqrt{B^2\cos^2\theta - \left(B^2 - R^2\right)}$$

$$D = B\cos\theta + \sqrt{B^2\cos^2\theta - B^2 + R^2}$$

$$D = B\cos\theta + \sqrt{B^2\left(\cos^2\theta - 1\right) + R^2}$$

Since $\sin^2 x + \cos^2 x = 1$

$$D = B\cos\theta + \sqrt{-B^2\sin^2\theta + R^2}$$

$$D = B\cos\theta + \sqrt{R^2 - B^2\sin^2\theta}$$

Now with two observations we can write an equation for the offset, *E*,

$$E = D\sin\theta$$

Therefore, we have our desired result

$$E = \sin\theta\left(B\cos\theta + \sqrt{R^2 - B^2\sin^2\theta}\right)$$

This result is correct for all angles and there are no approximations.

2.2.2. Data Collection

A circle (or a sphere) is characterized by its radius. A partial circle (an arc) is characterized by the radius of a circle that approximates its curvature at the given point: this is called the *radius of curvature*. Several techniques were used to measure the radius of curvature of the image of the gas bubble.

(1) The subject estimated and recorded the radius of curvature of the bubble by eye.

(2) A dozen hoops of wire were prepared with radii of 2, 5, 10, 15, 20 … 100 cm. The subject held various hoops at arm's length and selected the hoop that matched the curvature of the bubble's image. We recorded

the radius of this hoop in cm. An observer carefully watched to make sure that the subject was holding the hoop at arm's length.

(3) Just a few hoops of wire were prepared and the subject walked slowly toward a hoop and stopped when the radius of the hoop matched the radius of curvature of the bubble's image. We recorded the radius of the hoop in cm and the distance between the hoop and the subject's eye.

(4) The subject held a meter stick 57.3 cm from the eye and measured the diameter of the bubble.

(5) A circle was presented on a computer screen 57.3 cm in front of the subject and the subject adjusted the radius of the circle to match the radius of curvature of the bubble's image. This has been often easier if the subject was looking down at the monitor. This technique had the least variability. It also confirmed that the bubble outline was indeed a circle.

All of these measurements were taking in the morning with the subject's head upright. The pupil was always 3 by 4 mm, because a previous faulty cataract surgery had trapped the iris.

2.2.3. Human and Animal Rights

The author hereby declares that all experiments have been examined and approved by the appropriate ethics committee and have therefore been performed in accordance with the ethical standards laid down in the 1964 Declaration of Helsinki. The subject (the author) has given his informed consent for this report to be published.

3. RESULTS

On July 1, 2008, the ophthalmologist performed my second retinal detachment operation: he found two tears, pushed the macula back into place, zapped the retina with a laser and injected another gas bubble. He instructed me to sleep face down overnight and thereafter to lay on my right side with a pillow when convenient. The gas was absorbed over the next 73 days. Nine days after the operation, I saw something other than cloudy white unfocused fog. The first objects that I saw as the gas was absorbed were stars in the sky as shown in Figures 5 and 6. I was outdoors at night looking straight ahead.

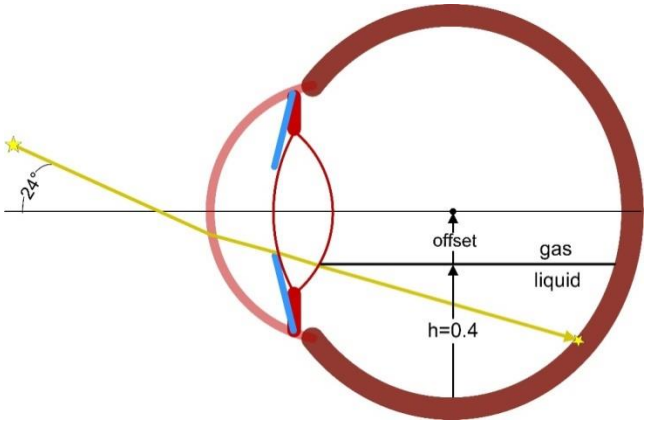

Fig-5. Side-view of the eye (sagittal section) showing the first rays of light that the subject saw after detached retina operations that injected perfluoropropane gas. The subject saw nothing until enough gas had been absorbed to allow a ray of light like this one to reach the retina in focus. Light rays that go through the gas bubble bend and scatter before they reach the retina. Only the rays that go through the aqueous humor can reach the retina in focus. The indicated ray is bent according to Snell's law of refraction at three surfaces: the cornea, the front of the intraocular lens and the back of the lens.

For a typical human eye in primary position, the eyebrow blocks light from objects than are more than 45 degrees above the horizon. For an eye filled with gas, no objects will be seen because of the index of refraction of the gas. Light rays that go through any part of the gas bubble bend and scatter before they reach the retina. Only the rays that go through the aqueous humor can reach the retina in focus. As the gas was replaced with liquid, there came a time when a ray of light was able to sneak through to the retina. For the diagram in figure 5, this occurred on day nine when the fluid height rose to 0.4 cm and a star 24 degrees above the horizon suddenly became visible. This computed datum point amazingly fits the later measured data shown in figures 6 and 7. The indicated ray is bent according to Snell's law of refraction at three surfaces: the cornea, the front of the intraocular lens and the back of the lens. Light from objects above this star had to pass through the gas and light from objects below this star were blocked by the iris. Position of the successful ray depended on the size of the pupil. However, we did not have to control for this, because, serendipitously, this subject's pupil was always 3 by 4 mm.

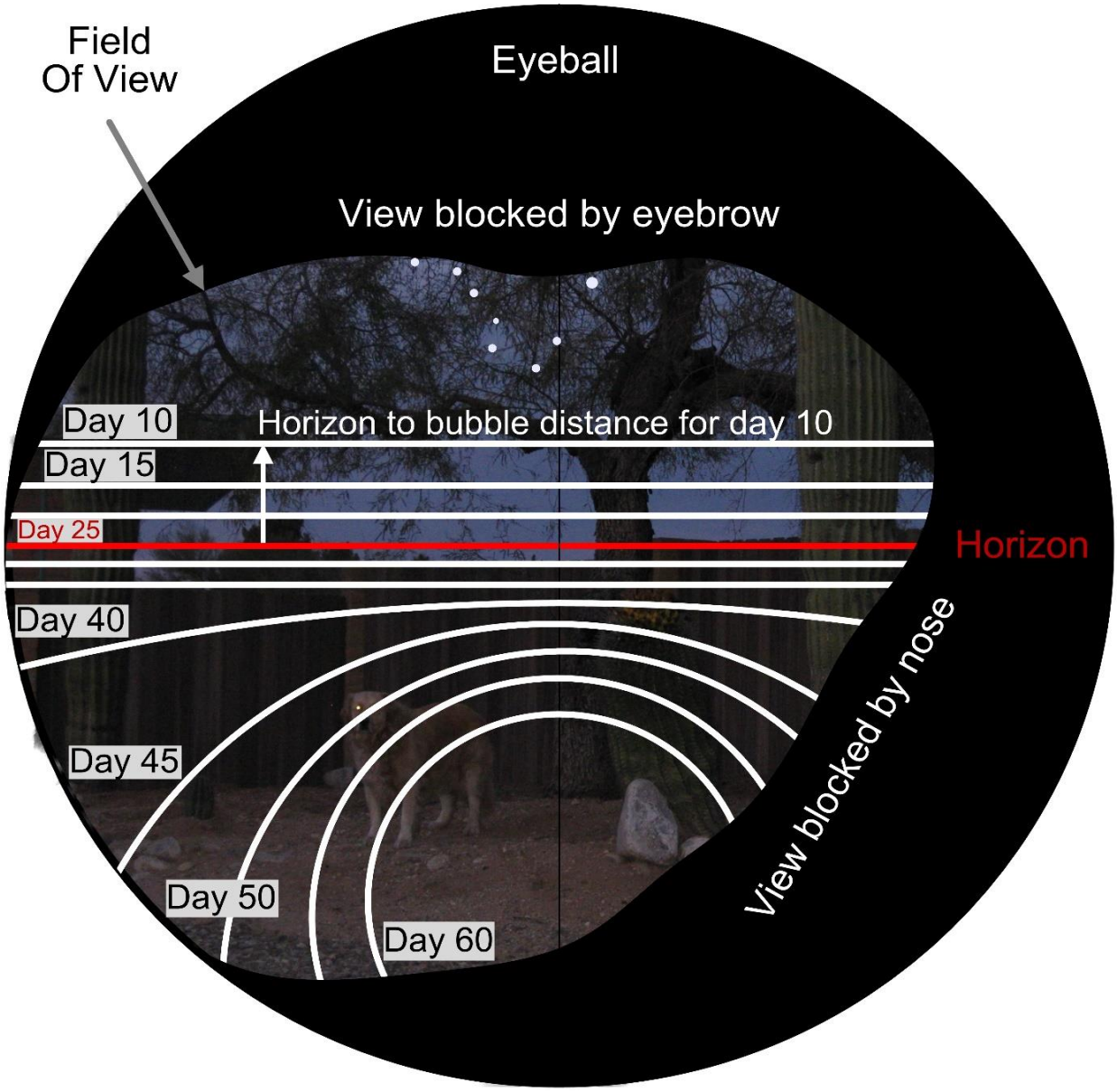

Fig-6. The subject's field of view showing daily changes in the subject's perception of the gas bubble being absorbed and replaced with aqueous humor. The white lines represent the surface of the gas-liquid boundary: the subject could not see below them for the indicated day. The figures in this paper are for physical configurations, meaning the top of the diagram corresponds to the top of the eyeball, as shown in this figure.

Figure 6 shows our subject's field of view (FoV) for an outdoor scene with the eye looking straight-ahead (primary position). Theoretically, the human could see ±90° in each direction without moving the eye. But, because the eyes are set back in the skull, our field of view is restricted. Typically, the human FoV is only 45° up (limited by the eyebrow), 65° down (limited by the cheek), 55° nasal (limited by the nose) and 90° temporal as shown in figure 6. By moving his head, the subject can see other objects. Figure 6 also shows how the bubble changed its size and shape as the gas continued to be absorbed into the blood via the retina and choroid.

Figure 6, which is unique in the ophthalmological literature, shows my viewpoint of the time sequence of the gas bubble being absorbed and replaced with aqueous humor. Because the gas was 100% perfluoropropane, in the days immediately after the operation, the gas bubble increased in size [7, 8] but I did not detect this, because I could only see a blurry white fog with shadows and bright areas. I could detect *where* a window was, but I could not see the window. On day 9, I was surprised to see something. It was a star and the bottom of the gas bubble. In figure 6, this gas-liquid surface looked horizontal, so I measured how far it was from the horizon. {Because the horizon was obscured by a part of the bubble, I used my vestibular system to estimate the location of the horizon.} In the next month, I saw many bizarre reflections off this gas-liquid surface, and some disturbed me. On each day, I could only see what was below the white line in figure 6 for that day. For, example, on the ninth day I could see stars; the surface of the bubble looked like a straight line 24 degrees above the horizon. On day 27, the gas-liquid surface crossed the horizon. Later, around day 40, the gas bubble started to look more like an arc and less like a line. So I started measuring the radius of curvature of the bubble. Eventually the bubble seemed to be a circle. For example, on day 55 it looked like a circle 22 degrees below the horizon with a radius of curvature of 25 degrees. We repeat that figure 6 is for one subject, with C_3F_8 gas and in only one operation although after my other two RD operations the gas bubble behaved the same way.

Range of the data. Because of the geometry of the eye and the bubble, for detached retina operations with an injected gas bubble, the largest measured offsets were +10, +19 and +24. The largest negative offsets measured were -34 and -43. The largest radii of curvature were 19, 35, 50 and 63.

A model is a simplified representation of one particular aspect of a physical system. To understand this philosophy the reader should compare the models of figures 2 to 6. Each models a different aspect of the eye. Each emphasizes details in one aspect and ignores details in other aspects. Figures 2, 3 and 4 explain the functions that transform the quantitative *input data* (horizon to bubble distance) into model parameters (the offset of the bubble surface from the center of the eye). Figure 5 shows how the gas bubble interferes with light rays. It shows *schematically* that the rays that hit the retina in focus depend on the source location, the size of the bubble and the size of the pupil. Figure 6 shows how the gas bubble affects vision. It shows how the size and shape of the gas bubble affects *images* of what the subject sees. These models show three independent aspects of the same physical system. They do not overlap. For example, the retina is in figures 2 to 5, but not in Figure 6. It is the independence of the submodels that makes the modeling powerful [9].

Figure 7 shows measured data from the subject's viewpoint of the temporal disappearance of the C_3F_8 bubble. The *horizon to bubble distance* starts on day 9 at about 24 degrees: this datum point is different than the rest, because it was computed from figure 5 not measured. This curve passes through zero on day 27. In this figure, data for the *radius of curvature* start on day 39 and decrease until the bubble completely disappeared on day 73. On the 60^{th} day, the bubble broke up into one big bubble and many little ones: from this day forward, the numbers for the radius of curvature are for the big bubble.

If volume data for days 40 to 60 were fit with an exponential, then the half-life would be 5.3 days. This compares favorably with [8] who stated that the half-life for absorption of C_3F_8 gas is about five days. {The half-life for days 1 to 73 was 10 days.}

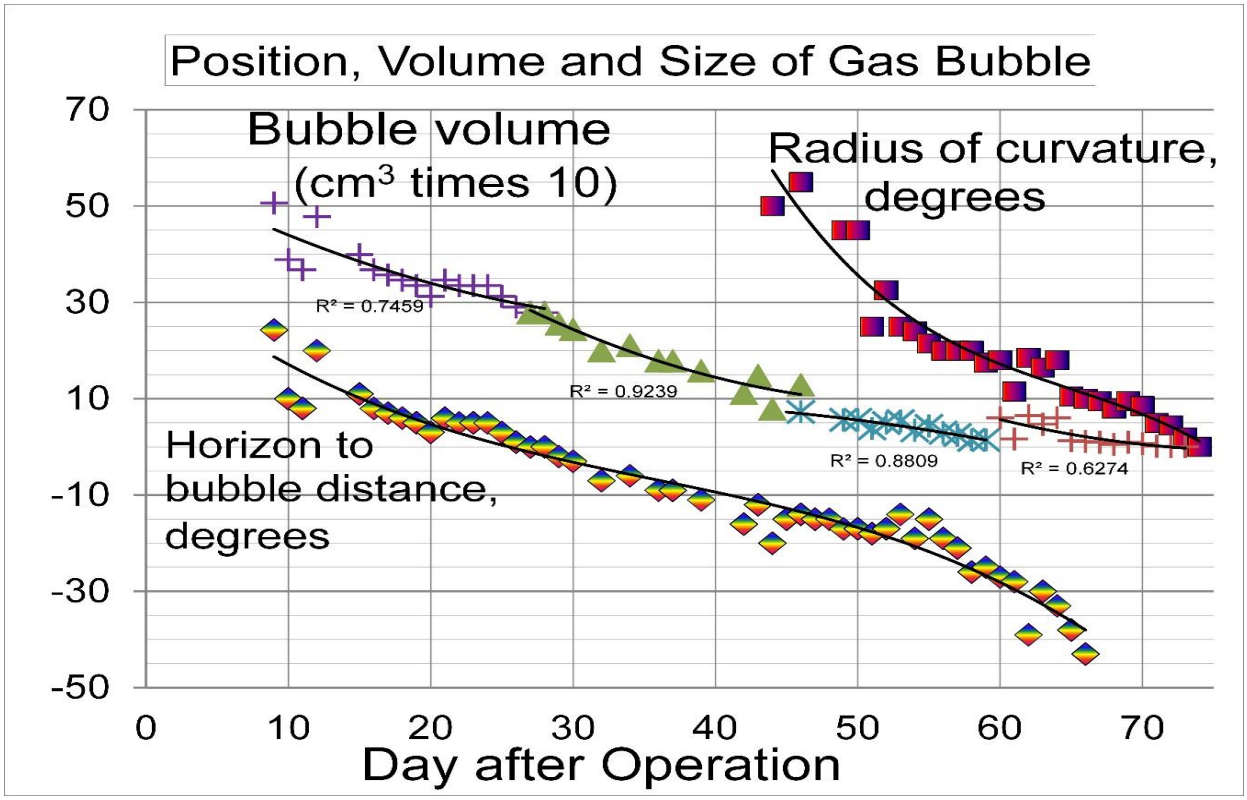

Fig-7. The subject's measurements of the gas bubble being absorbed and replaced with aqueous humor. The units for the *horizon to bubble distance* and the *radius of curvature* are degrees or cm: they are the equal because the target was 57.3 cm from the eye. The bubble volume was computed for the four geometric models: it has units of cm^3. Time is in days.

The *horizon to bubble distance* (in degrees or cm) is the absolute value of the distance above or below the horizon of the surface of the bubble. Because the visual target was 57.3 cm from the subject, one cm equals one degree. The horizon to bubble distance was transformed into the *offset* in cm of physical eyeball space, as shown in figure 2, using equations given in section 2.2.1. Units of degrees were used for the plots and units of centimeters were used for the volume calculations. The curves of figure 6 were based on the trend lines fit to the data of figure 7. Figure 7 also shows the *volume* of the bubble computed from the physical measurements. That is the topic of the next section.

The outputs of our data collection efforts were date (converted to day after gas injection and shown as the abscissa of figure 7), horizon to bubble distance (the left curve in figure 7), radius of curvature of the bubble (the right curve in figure 7) and comments. These were the inputs for our modeling efforts described in the next section.

3.1. Modeling the Geometry of the Gas Bubble

We developed a model for the change in position and volume of an intraocular C_3F_8 gas bubble as the gas was absorbed. However, because of the complex geometry of the bubble, we found that one model was not sufficient: therefore, we developed four submodels, one for each of the distinct bubble configurations. For all of these models, we assumed that the top of the gas bubble was in contact with the top of the eyeball (the bubble floats).

3.1.1. Model-1 Flat Surface in Lower Hemisphere

For days 1 to 28, the boundary between the gas and the aqueous humor liquid appeared flat, horizontal, and in the lower hemisphere. Therefore, a sphere (the eyeball) intersected by a plane is an appropriate model as shown in the top

of figure 8. The volume of the gas bubble is the volume of the sphere minus the volume of the spherical cap (the aqueous humor in the bottom).

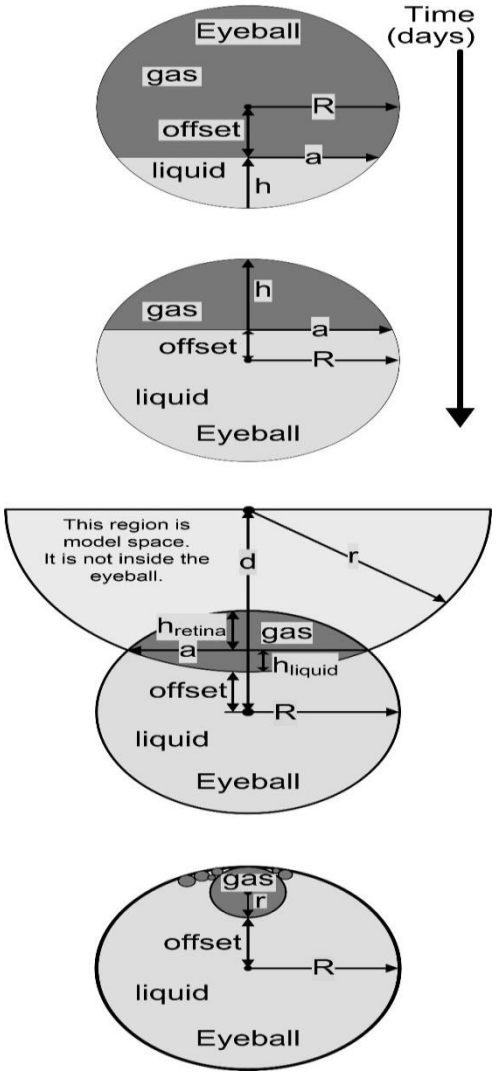

Fig-8. Vertical cross-sections (coronal sections) for the four gas-bubble configurations, from top to bottom: Model-1, the boundary between the gas and the aqueous humor liquid is a flat horizontal surface in the lower hemisphere. Model-2, the gas-liquid boundary is a flat horizontal surface in upper hemisphere. Model-3, the gas-liquid boundary is meniscus shaped and the gas volume is lens shaped. Model-4, the gas is contained in multiple bubbles.

For this model, R is the vertical radius of the eyeball, which is assumed 1.1 cm for our subject. The *offset* is computed from the subject's measure of the horizon to bubble distance. In this section, all numbers will be positive: the variables are scalars not vectors. The height (*h*) of the intersecting plane from the bottom of the sphere is computed with $h = R - offset$.

The volume of the spherical cap is $V_{\text{cap}} = \frac{\pi h^2}{3}(3R - h)$.

So, the volume of the gas bubble is $V_{\text{bubble}} = V_{\text{sphere}} - V_{\text{cap}} = \frac{4\pi}{3}R^3 - \frac{\pi h^2}{3}(3R - h)$.

{Alternatively, $V_{\text{cap}} = \frac{\pi h}{6}(3a^2 + h^2)$, where *a* is the radius of the intersecting disk, $a = \sqrt{h(2R - h)}$. When possible, we used alternative equations for verification.}

The surface area of the gas-liquid boundary is the area of the intersecting disk, $SA_{\text{disk}} = \pi a^2$. These equations are from http://mathworld.wolfram.com/SphericalCap.html. When the bubble surface reached the horizon ($offset = 0$), we switched to Model-2.

3.1.2. Model-2 Flat Surface in Upper Hemisphere

For days 27 to 44, the gas-liquid surface still seemed to be flat and horizontal, but now it was in the upper hemisphere as shown in the second part of figure 8. A sphere intersected by a plane is still appropriate; however, because the boundary is in the *upper* hemisphere, we needed new equations. In this new model, the gas bubble *is* the spherical cap.

R is still the radius of the eyeball. The height (*h*) of the intersecting plane to the top of the sphere is again computed with $h = R - offset$.

Now this time the volume of the spherical cap is the volume of the gas bubble. $V_{\text{cap}} = V_{\text{bubble}} = \frac{\pi h^2}{3}(3R - h)$.

{Alternatively, $V_{\text{cap}} = V_{\text{bubble}} = \frac{\pi h}{6}(3a^2 + h^2)$, where $a = \sqrt{h(2R - h)}$ }.

The surface area of the gas-liquid boundary is again the area of the intersecting disk, $SA_{\text{disk}} = \pi a^2$. In this period, the gas-liquid surface started to curve into a meniscus shape, so we segued into model-3. However, there was no sharp point of transition.

3.1.3. Model-3 Curved Meniscus-Shaped Surface

For days 45 to 59, the gas-liquid surface was curved in a meniscus shape, caused by surface tension [7]. So the gas bubble surface was modeled with a sphere of which only a portion was inside the eyeball, as shown in the third part of figure 8. A model for the volume of the gas bubble is that of the intersection of two spheres: one for the eyeball and one for the extended bubble: this volume is lens shaped.

R is the radius of the eyeball (1.1 cm) as before, the $offset$ is the distance between the center of the eyeball and the gas-liquid boundary, *r* is the radius of curvature of the gas bubble (in cm) and *d* is the distance between the centers of the spheres, $d = r + offset$. We have data for these, because *r* and *offset* are input parameters. The equations in this section are based on Weisstein [10].

They are only valid if $d < R + r,$ otherwise there would be no intersection. Substituting $d = r + offset$ yields condition-1 $0 < offset < R.$ Next, $d < R - r,$ otherwise one sphere would be completely inside the other. Knowing that $d = r + offset$, yields condition-2 $-0.5offset + 0.5R < r$.

The volume of the intersection of two spheres is the sum of the volumes of two spherical caps.

$$V = \frac{\pi}{3}\left[h_{\text{retina}}^2 \left(3R - h_{\text{retina}}\right) + h_{\text{liquid}}^2 \left(3r - h_{\text{liquid}}\right)\right]$$

Figure 8 (middle) illustrates the definition of h_{liquid}, which is the distance from the intersecting disk to the aqueous humor and h_{retina}, which is the distance from the intersecting disk to the retina.

An alternative form for the volume equation is

$$V = \frac{\pi(R + r - d)^2 (d^2 + 2dr - 3r^2 + 2dR + 6rR - 3R^2)}{12d}$$

Let us now compute the surface area of the gas-liquid boundary. This time we do not want the area of the intersecting disk, but rather we want the area of the curved side of the spherical cap. First, we need the distance of the gas-liquid boundary from the plane of intersection of the two spheres.

$$h_{\text{liquid}} = \frac{(\text{R} - r + d)(\text{R} + r - d)}{2d}$$

Now we can use the formula for the surface area of the curved side of a spherical cap $SA_{\text{cap}} = 2\pi r h_{\text{liquid}}$

{The intersection of two spheres is a circle with radius *a*. So, alternatively, we can write the gas-liquid surface area as

$SA_{\text{cap}} = \pi(a^2 + h_{\text{liquid}}^2)$ with $a = \frac{1}{2d}\sqrt{[4d^2R^2 - (d^2 - r^2 + R^2)^2]}$.}

The transition from model-3 to model-4 was easy to identify, because the subject said something like, "Whoa, the bubble broke up into multiple bubbles."

3.1.4. The Missing Model

It seemed reasonable for the gas bubble to transition from model-3, the lens-shaped bubble, into a single spherical bubble and then break up into multiple bubbles. However, in four observed bubble absorptions, this model geometry was never seen. The bubble always went from the lens-shaped bubble directly to multiple bubbles.

Furthermore, the criterion for a single bubble $R-offset-2r=0$ never occurred in the data. It may be that this configuration was fleeting because the surface area of gas in contact with the retina was so small.

3.1.5. Model-4 Multiple Bubbles

For days 60 to 73, the gas had broken up into multiple bubbles. Therefore, we needed a model for many different sized bubbles. However, I had only collected data for the big bubble. Therefore, the match for this section is not accurate. Most surprisingly, seven years later, I had a detached retinal in the right eye. This time I recorded sizes of all the bubbles. It confirmed that only the large bubble was necessary to model the volume and the surface area,

The volume of the gas is approximately $V_{\text{bubble}}=\frac{4\pi}{3}r^3$, where *r* is the radius of the main bubble.

The surface area of the gas-liquid boundary is approximately $SA_{\text{gl}}=4\pi r^2$ although the actual surface area would be larger due to the multiple bubbles.

To show the reasonableness of the model-4 approximation, we note that for one particular day we have data for the individual bubbles. On day 63, there were six bubbles with diameters of 1, 1, 2, 2, 8 and 33, which yield a total volume of 0.484 ml and a total surface area of 3.16 cm^2. As expected, these numbers are slightly larger than the model-4 approximations (only one bubble of 33 degrees) of volume 0.477 ml and surface area 2.95 cm^2.

[11] plotted human intraocular bubble volume (ml) versus the angle of retina-gas contact (degrees). Their data for small volumes was fit with the equation $Vol=0.02\theta-0.5$. This was used to give the gas-retina contact area with $CA_{gr}=\pi\left(\frac{R\theta}{2\times 57.3}\right)^2$.

Figure 7 presents the input data: the horizon to bubble distance and the radius of curvature of the bubble. Figure 7 also presents the outputs of the four submodels. The discrete symbols in the volume path are the outputs of the four individual models and the trend lines are the best-fit equations to those data, which were fit with exponentials, straight lines, logarithmic functions, power functions and polynomials. For model-1, model-2 and model-3 second-order polynomials gave the best fit to the data.

3.2. Select Valid Segments and Compute Best Fit

Now came the moment of truth. We needed to determine if these four geometric models were consistent with each other. There was no *a priori* reason to expect them to be so, because the data were collected with no preconceived model in mind. To examine this possible consistency, we selected the segments when each of the four models was valid: for example, the output of model-4, multiple bubbles, was only valid for days 59 to 73. These four valid segments are shown in the volume path of figure 7 with different symbols and different trend lines. Surprisingly, each model intersected well with the next model. Sometimes the valid segments overlapped for a few days before diverging. In the next step, the overlapping portions were resolved and we choose a single continuous string of volume estimates 73 days long, shown in figure 9 with big brown $\times$ symbols.

Table-1. Valid and chosen range of days

	Valid range of days derived from figure 5.	R^2	Chosen range used in figure 11.
Model-1	1-28	0.72	1-27
Model-2	27-46	0.92	28-45
Model-3	46-59	0.88	46-59
Model-4	60-73	0.76	60-73

Source: author's data

The volume data of figure 9 were fit the best with the second-order polynomial $V = 0.0007t^2 - 0.13t + 5.6$ where V is in ml and t is in days. Figure 9 also shows the surface area of the gas-liquid boundary and the contact area of the gas-retina interface.

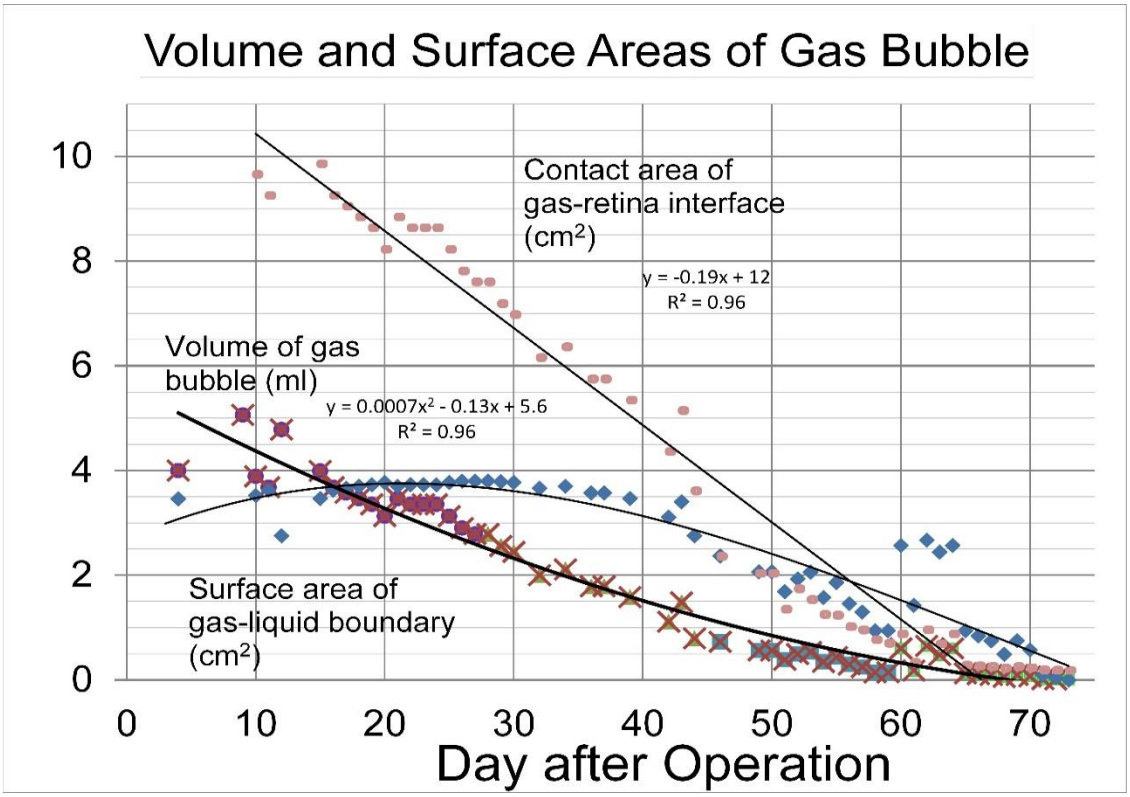

Fig-9. Volume, the gas-liquid surface area and the gas-retina contact area as the gas bubble is absorbed and replaced with aqueous humor. Volume has units of milliliters (ml) or cm^3. Surface area has units of cm^2. Time is in days

3.3. Compute Gas-Retina Contact Area

The aspect represented by our previous models was the surface area between the C_3F_8 gas and the aqueous humor. The following four alternative models investigate the aspect of the contact area between the C_3F_8 gas and the retina, which is the other side of the sphere from the gas-liquid boundary.

Model-1b, Flat horizontal surface in lower hemisphere

The contact area of the gas-retina interface is $SA_{\text{sphere}} - SA_{\text{cap}} = CA_{\text{gr}} = 4\pi R^2 - 2\pi Rh$

Model-2b, Flat horizontal surface in upper hemisphere

The contact area of the gas-retina interface is $SA_{\text{cap}} = CA_{\text{gr}} = 2\pi Rh$.

Model-3b, Meniscus shaped surface

The contact area of the gas-retina interface is $CA_{\text{gr}} = 2\pi Rh_{retina}$, where

$$h_{retina} = \frac{(-R + r + d)(R + r - d)}{2d}.$$

Model-4b, Multiple bubbles

The contact area of the gas-retina interface is $CA_{gr} = \pi\left(\frac{R\theta}{2\times 57.3}\right)^2$, where $\theta = 50Vol + 25$

Data for these four alternative contact area models are plotted in figure 9 with pink disks.
Which of these modeling strategies (gas-liquid surface area or gas-retina contact area) best match the time rate of change of the volume data?

3.4. The Dynamic Component

Our model for intraocular gas absorption has two components, structure and dynamics (see figure 10). The structure is comprised of the four geometric configurations (with accompanying equations) that a bubble goes through in its lifecycle. These four submodels were used to produce the four segments of the gas volume data of figure 7. Then the overlapping portions were resolved and we created the single continuous string of volume estimates 73 days long, shown in figure 9. We also found the equation that best fit those data.

Now, we want to develop the dynamic component of our model for the absorption of the intraocular gas bubble. The system being modeled is the gas bubble, the aqueous humor and their functional behavior. The system input is the aqueous humor that is being made by the ciliary body. The outputs are the aqueous humor that is draining out of the anterior chamber primarily through the trabecular meshwork (which for the absorption phase must be less than the aqueous humor being produced by the ciliary body) and the gases (C_3F_8, N_2 and O_2) that are absorbed by the choroid and the blood. First, we looked at the three alternative differential equations for this model that had been proposed in the literature.

1. Would a differential equation like $\frac{dV}{dt} = -kV$ be a good model for the volume of the perfluoropropane gas shown in figure 9? This was one of the earliest mathematical models [12] for intraocular gas absorption. However, the solution to that equation is an exponential equation and an exponential never reaches zero: furthermore, the best exponential fit to these data is $V = 15e^{-0.07t}$, where V is in cm^3 and t is time in days. The coefficient of determination for this equation is $R^2 = 0.83$, which is not a good fit, and the initial value is 15 which far from the actual value of 4 ml on day 4.

2. Would a differential equation like $\frac{dV}{dt} = -kSA_{gl}$, where SA_{gl} is the surface area of the gas-liquid boundary (in cm^2), be a good model for the rate of change of volume? This is the model suggested by Woon, et al. [13] who wrote that, Our "results show that the rate of absorption contains a term in time squared, indicative of absorption through the exposed surface area of the aqueous humor [SA_{gl}] rather than via the exposed retina[CA_{gr}]." The mathematical symbols SA_{gl} and CA_{gr} were added to the quote. However, the surface area of the gas-liquid boundary curve (fit to the rotated blue squares in figure 9) starts with a positive slope (especially if the bubble completely fills the eye in the beginning), peaks in the middle and then falls with a negative slope, unlike the monotonic decreasing slope of the volume data. More significantly, the fatal flaw in this model is that if in the beginning the eye were completely filled with gas, then there would be no gas-liquid boundary and the gas volume could never change.

3. Finally, would a differential equation like $\frac{dV}{dt} = -kCA_{gr}$ where CA_{gr} is the contact area of the gas-retina interface (in cm^2) [9] be a good model for the volume data? Yes. First, it produces a volume curve that *does* reach zero, unlike the exponential. Next, we let Excel fit exponentials, straight lines, logarithmic functions, power functions and polynomials to the volume data of figure 9. The overall best[1] fit was the second-order polynomial

$V = 0.0007t^2 - 0.13t + 5.5$ where V is in ml or cm^3 and t is in days, with $R^2 = 0.96$. We computed its time derivative (slope) as $\frac{dV}{dt} = 0.0014t - 0.13$, which is monotonic decreasing as required by the data (for $t < 86$ days). Next we looked at the contact area of the gas-retina interface line (fit to the pink disks in figure 9) to see if it could be our solution. The best fit to these data is the straight line $CA_{gr} = -0.19t + 12$ with $R^2 = 0.96$. Now if we let $k = \frac{-0.01 \text{ cm}}{\text{day}}$, then we get $kCA_{gr} = 0.0019t - 0.12$. This is remarkably similar to the time derivative (slope) of the volume equation given above.

In summary, we investigated dozens of solutions for fitting the measured gas volume data given in figure 9. The equation that gave the best fit for the whole data set is the second-order polynomial $V = 0.0007t^2 - 0.13t + 5.5$, with its time derivative of $\frac{dV}{dt} = 0.0014t - 0.13$. Next, we approximated this derivative with the gas-retina contact area equation of $kCA_{gr} = 0.0019t - 0.12$. This finally allowed us to write the system dynamics equation of

$\frac{dV}{dt} = -kCA_{gr}$, where CA_{gr} is the contact area of the gas-retina interface.

This, then, is our final complete model for the absorption of an intraocular perfluoropropane gas bubble injected during a retinal detachment operation.

4. DISCUSSION

When a 12% to 16% concentration of C_3F_8 gas is used, model-1 is fine. However, when a 100% concentration of C_3F_8 is used, the gas bubble has three phases [3]; [5]; [4]; [6]; [13]; [15]. In the beginning, the concentration gradients of the gasses are large: the bubble is 100% C_3F_8 with zero O_2 and N_2. Whereas, the blood has zero C_3F_8 but a large amount of O_2 and N_2. Of these three gasses, O_2 diffuses the fastest and C_3F_8 diffuses the slowest. So for the first few days the bubble expands to about four times its original size, because O_2 and N_2 diffuse in at a rapid rate. Finally, the

[1]Best in the sense of highest R^2, smoothness of transitions and, by Ockham's Razor, the least complexity. The principle of Ockham's (or Occam's) Razor states that if two models are equal in all respects except complexity, then the simpler model is better [14]. This explains how a second-order polynomial can be better than a sixth.

diffusion gradient for O_2 and N_2 reaches zero. The bubble now stays in this equilibrium phase for a few hours. Thereafter, it enters the contraction phase and C_3F_8 diffuses out of the bubble and into the blood. The expansion phase was not included in model-1, because our subject saw nothing until day nine. However, we did enter an initial condition for the volume in the expansion phase of 4 ml on day 4, based on the surgeon injecting 1 ml of C_3F_8 into a 5 ml virtuous cavity: this gas quadruples in size in three to four days. This datum point strikingly fits the later measured data. This paragraph is actually model-0.

Figure 6 might not be the first illustration of a subject's view of a disappearing C_3F_8 gas bubble. The abstract of a three page French language paper [16] states that it contains an analogous description.

4.1. Risk Analysis

Why is it important to know how long an intraocular gas bubble will last? The patient and the surgeon need this information to plan their futures. While a gas bubble is inside the eye, the patient must not ride a gondola to the top of a high mountain or fly in an airplane (even if the cabin pressure were kept below the legal limit of 8,000 feet), because *de*creased external atmospheric pressure would expand the intraocular gas bubble in the closed globe. This in turn would increase the intraocular pressure and possibly restrict the central retinal artery. Our model would respond with neuronal control that would decrease active secretion of aqueous humor by the ciliary body and with increased intraocular pressure that would increase the amount of aqueous humor that is draining out of the eyeball primarily through the trabecular meshwork [17]. But this would take time: it cannot do this fast enough to avoid harm in *all* people. "It is likely that most patients with a bubble of ≤1 mL could safely fly with standard cabin pressurization [18]." Our patient's bubble became <1 mL on the 45th day. The alternative compensation mechanism for lower pressure would be to increase the absorption rate for the gases (C_3F_8, N_2 and O_2) that are being absorbed by the choroid and the blood. But this is a diffusion process and is not controllable.

On the other side of the pressure range, the patient must also avoid *in*creases in external pressure. The patient must not dive into water or do anything else that would increase the surrounding pressure. Even routine activities like swimming might be restricted, because submerging an eye 16 inches without goggles would increase the intraocular pressure by 30 mm Hg, which might be dangerous. If a patient with a gas bubble went scuba diving, the extraocular pressure would increase. The eye would gradually increase the production of aqueous humor to compensate. Then when the diver ascended to the surface the external pressure would return to sea level and the intraocular gas would expand producing intraocular pressures of 50 mm Hg or more.

Both the patient and the surgeon must ensure that nitrous oxide anesthesia is not used if any residual gas remains in the eye. Nitrous oxide (N_2O) is a common anesthetic used by anesthesiologists and dentists. However, because of its solubility in blood, if it were given to a patient with an intraocular gas bubble, it would diffuse into the eyeball at least twenty times faster than the intraocular gasses (O_2, N_2 and C_3F_8) could diffuse out. This would increase the intraocular pressure, which would displace the iris and lens anteriorly, which would restrict the outflow channel for intraocular aqueous humor. Together, these effects would block blood flow in the central retinal artery, which could cause permanent blindness [19].

For planning, the RD patient should be aware that the average rate of absorption in the beginning of the bubble's lifecycle, for example days 10 to 20, was -0.1 cm^3/day, whereas the average rate of absorption near the end, for example days 60 to 70, was -0.05 cm^3/day, which is half the speed. This means that RD patients must be very patient in the last weeks of the gas bubble lifecycle. For planning trips and other activities, we offer the following rule of thumb, when the bubble surface got to the horizon, my bubble lifecycle was one-third of its way to completion.

Other risks associated with vitrectomy and injection of intraocular gasses (but not related to the model) include infection, retinal re-detachment, chronic high or low intraocular pressure, macular edema, retinal hemorrhage, development of a cataract, and adhesions (synechiae) of the iris to spots along the edges of an intraocular artificial lens.

4.2. Future Improvements

Model-1 is strong. If the injected intraocular gas is C_3F_8 with a concentration around 15%, then there is no reason to change model-1. If the injected gas is 100% C_3F_8, then some gas volumes could be calculated for the first few days but measurements could not be made. Model-2 is a simplification of model-3. Model-3 could be improved if the subject started collecting radius of curvature data when the gas-liquid surface reached the horizon. However, I was not able to discern this curvature for another two weeks. If the gas-liquid surface is flat, meaning that the radius of curvature is infinite and the gas bubble is hemispheric, then all equations of model-3 reduce to the equations of model-2. Model-4 could be improved if the subject recorded the sizes of all the bubbles.

The model validity conditions could used to help verify data collection. The *offset* increases with time, but for model-3 to be valid, it must satisfy condition-1 $0 < offset < R$. Similarly, the radius of curvature, *r*, decreases with time, but for model-3 to be valid it must satisfy condition-2 $-0.5offset + 0.5R < r$. Therefore, these conditions could be checked when input data were being collected to make sure that the data were errorless.

Making any of these changes is at the discretion of the modeler. He or she must trade off complexity for accuracy.

A powerful model verification technique is running a model backward in time. If we had a numerical simulation or a physical analog of the eyeball, then we could switch the inputs and outputs and run the model backwards. The output gases (C_3F_8, N_2 and O_2) that are absorbed by the choroid and the blood would become inputs injected into the top of the eyeball. The input aqueous humor that is coming in from the ciliary body would be reversed to become the output from the front of the eyeball through the trabecular meshwork. Then, we would observe if the gas bubble goes through the four model configurations shown in this paper. Of course, flow rates and pressures would have to be adjusted.

4.3. Possible Level Changes

> "Most systems are impossible to study in their entirety, but they are made up of hierarchies of smaller subsystems that can be studied. Herb Simon [9] discussed the necessity for such hierarchies in complex systems. He showed that most complex systems are decomposable, enabling subsystems to be studied outside the entire hierarchy. For example, when modeling the movement of a pitched baseball, it is sufficient to apply Newtonian mechanics considering only gravity, the ball's velocity and the ball's spin [20]. One need not be concerned about electron orbits or the motions of the sun and the moon. Forces that are important when studying objects of one [level] seldom have an effect on objects of another [level] [21]."

Would it help our present model if we added a fluid dynamics model for the flow of fluid out of the trabecular meshwork, as suggested by reviewer? No, it would increase the complexity level above the rest of the model. Would it help our model if we investigated alternative pathways for gas absorption through the aqueous liquid and out via the uveoscleral drainage or the trabecular meshwork? No, it would increase the complexity level, but the changes to the model's behavior would be insignificant.

The lowest level of accuracy in our model is the data measured by our subject for the *horizon to bubble distance* and the *radius of curvature* of the gas bubble. By looking at figure 7, one could surmise that the data are accurate to at best ±1 degree. Anything that would increase the level of accuracy of these measurements, such as telling the subject how close his measurements were to the three limiting conditions, should be helpful. These three limiting conditions are condition-1 $0 < offset < R$, condition-2 $-0.5offset + 0.5R < r$ and condition-3 $R = offset + 2r$. Telling the subject about these conditions while data were being collected would help ensure that the data were consistent.

Listing's reduced eye model given in figure 2 is simple. It was used throughout our study, with one exception: when it was necessary, as in figure 5, we used a more complicated ray-tracing model. Would it help if we used the ray-tracing model throughout? No, it would raise the level of accuracy and complexity, however, it would not produce notable changes in the behavior of the model, because the changes would be smaller than noise in the input data.

The volume data of figure 7 were fit with second-order polynomials. Would easily available sixth-order polynomials fit the data better? Yes, they would increase the level of accuracy, but the R^2s being away from 1.0 are not due to inadequacy of the polynomials. It is due to noise in the input data. So sixth-order polynomials would not improve the model.

How could we know which parameters could change the figures, results or conclusions of the model? We could do a sensitivity analysis [22]. Table 2 shows the results of a sensitivity analysis for the eyeball radius and the intercept of the bubble volume versus the contact area equation. The sensitivity analysis of Table 2 was designed to answer the question, "What would make the gas-retina contact area equation match the derivative of the volume better?" The two choices are changing the model radius of the eyeball by 10% or changing a parameter in the formula for computing the gas-retina contact area for model-4. The parameter we are referring to is the intercept of the data of Hilton and Grizzard [11]. They plotted the intraocular bubble volume (ml) versus the angle of retina-gas contact (degrees). Their data for small volumes was fit with the equation $Vol = 0.02\theta - 0.5$. Model-4 used this equation to get the gas-retina contact area. The middle row of Table 2 has the normal values for the eyeball radius (1.1 cm) and the contact area intercept (-0.5 ml). The top row changes the intercept value by 10%. The bottom row changes the eyeball radius by 10%. Changing the radius had a greater effect on matching the equations than changing the intercept did. Therefore, in terms of matching the gas-retina contact area equation and the derivative of the volume equation, the radius of the eyeball is more important than the intercept in the intraocular bubble volume versus the angle of retina-gas contact equation.

The data in this study were collected by the subject recording only two easily measured parameters, namely the horizon to bubble distance and the radius of curvature of the bubble. It is not known if better data could be collected with other techniques such as the ophthalmologists' view through an ophthalmoscope, the view through a slit lamp, optical coherence tomography (OCT) images, fundus photos, visual field diagrams or Optomap images [2, 7]. These other techniques might also work for the first couple of days before the bubble surface became visible.

Table-2. Sensitivity analysis

Condition	Radius (cm)	Intercept (ml)	Best fits to the data
Intercept decremented by 10%	1.1	-0.55	$CA_{gr} = 0.0018t - 0.1226$ $dv/dt = 0.0014t - 0.13$
Normal	1.1	-0.5	$CA_{gr} = 0.0019t - 0.1229$ $dv/dt = 0.0014t - 0.13$
Radius decremented 10%	1.0	-0.5	$CA_{gr} = 0.00155t - 0.10$ $dv/dt = 0.00160t - 0.12$

Source: author's data

Using these techniques might improve the fit of the model. The weakest link in the model is the accuracy of the subject's measurements: it was not the accuracy of our computations or physical parameters. Anything that could improve the weakest link would be worth pursuing. These changes might increase the level of accuracy of the input data. This would be beneficial, because it would raise the level of accurately of the whole model.

Changes that increase the level of complexity of a model, without changing the results or conclusion, would make the model more complex and therefore worse. Changes that *reduce* the level of complexity were *never* suggested by any reviewers. The following examples that increase the level of complexity were *actually* suggested by reviewers of this paper:, alternate pathways for gas absorption through the aqueous liquid and out via the trabecular meshwork and the uveoscleral drainage, a fluid dynamics model for fluid flow in the trabecular meshwork, finite element analysis, more sophisticated data analysis, ray-tracing for all analysis, parameters that match the consensus values on the Internet, and more complex mathematical analysis. These changes would change the level of parts of the model and would therefore be detrimental.

When considering changes in a model a cost to benefit analysis should be performed. Changing levels of any aspects are definite costs that must be balanced with potential befits. It is very important that the modeler refuse to add superfluous changes that would make the physiology more accurate, but would not improve the model.

In conclusion, some changes could improve our model and some would make it worse. Only changes that reduce the variability of the input data would improve the model, because the input data are the weakest link.

"Numquam ponenda est pluralitas sine necessitate," which can be translated as,

Never posit complexity without necessity – Ockham's Razor

"A scientific theory should be as simple as possible, but no simpler." – Albert Einstein

"A model should be as complex as necessary, but not more complex." – Terry Bahill

"As simple as possible, as complex as necessary." -- Ernst Schmutzer,

4.4. Dénouement

Our overall model has two components, one for structure and one for dynamics.

Structure was investigated with three alternatives

1. Geometric models with equations for the gas volume, figure 8.
2. Geometric models with equations for the gas-liquid surface area, models-1 to 4.
3. Geometric models with equations for the gas-retina contact area, models-1b to 4b

Dynamics of the gas absorption rate was investigated with three alternatives

1. $\frac{dV}{dt} = -kV$ The rate of change of bubble volume was proportional to the volume.
2. $\frac{dV}{dt} = -kSA_{gl}$ The rate of change of bubble volume was proportional to the gas-liquid surface area.
3. $\frac{dV}{dt} = -kCA_{gr}$ The rate of change of bubble volume was proportional to the gas-retina contact area.

The data in figure 9 were best fit with an equation of the form $\frac{dV}{dt} = -kCA_{gr}$, where CA_{gr} is the contact area of the gas-retina interface.

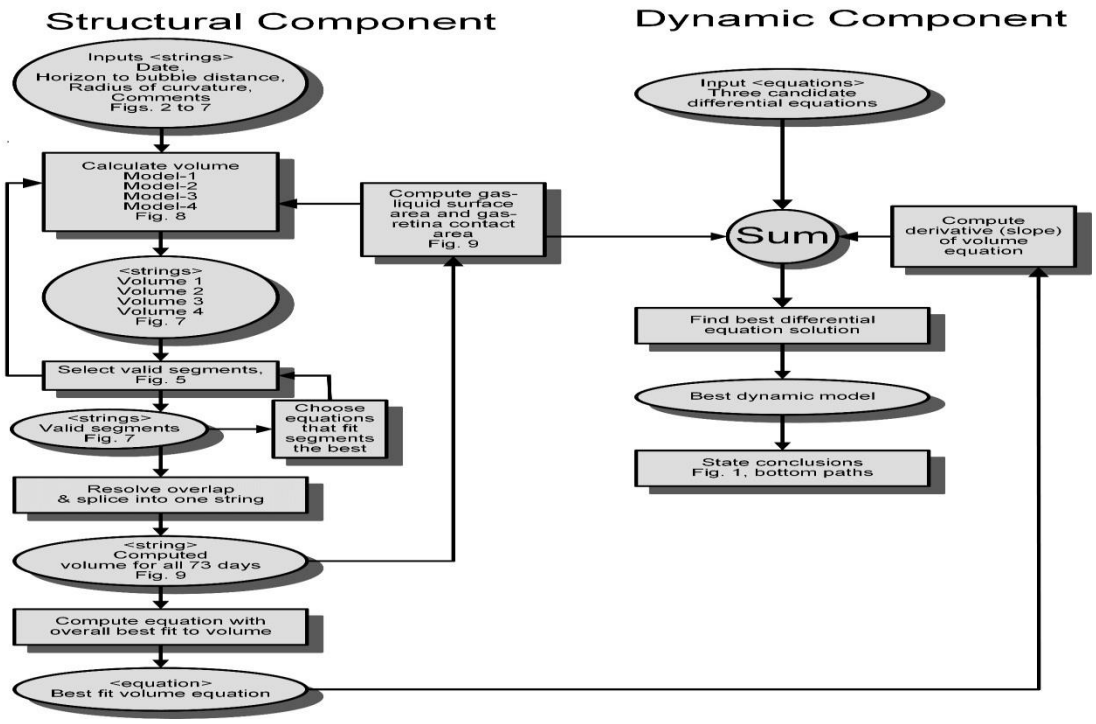

Fig-10. Functional flow block diagram of the process used in this study. The rectangles contain *functions* that were performed and the ovals contain *objects* that were produced. There is an alternation of input-function-output tuples.

Figure 10 is a roadmap for the process that we followed in this study. It starts with the four inputs to the system, which are strings (columns in a spreadsheet): (1) the date, which was immediately converted into the number of days since the intraocular gas injection, which runs from 1 to 73, (2) the horizon to bubble distance that was measured by the subject almost every day, (3) the radius of curvature of the surface of the bubble and (4) comments that the subject recorded, such as, "Whoa, the bubble broke up into multiple bubbles." These inputs are explained with figures 2, 3, 4 and 6. These inputs were put into the four geometric models (figure 8) and the models calculated four candidate volume strings. Next, we selected the segments when each model was valid, for example, the output of model-4, multiple bubbles, was valid only for days 59 to 73 and no model was valid for days 1 to 8, figure 5. These four valid segments are shown with different symbols and trend lines in the volume string of figure 7. Sometimes these segments overlapped for a few days. In the next step, the overlapping potions were resolved and we computed a single continuous string of volume estimates 73 days long shown in figure 9. A second-order polynomial gave the best fit to these data. Figure 9 also shows the surface area of the gas-liquid boundary and the contact area of the gas-retina interface. That completes the structural component of our model. To create the dynamic component, we used outputs from the structural component and three differential equations that had been suggested in the literature. Then we found the best differential equation solution. This gave us the best dynamic model for the absorption of intraocular gas. The bottom information flows of figure 1 were exercised when we suggested that in the physical system the time rate of change of gas volume is most likely proportional to the amount of gas in direct contact with the retinal surface.

4.5. Post-Surgery Checklist

Retina surgery patients do not know what to expect after their operations. The foreseeable experiences are too variable to be described in a single brochure. And the retinal surgeon does not have the time to explain all of the relevant possibilities to each patient. Therefore, it would be helpful to the patient if, immediately after an operation, the surgeon dictated answers for questions like these.

What is the patient's name? What was the date of the operation? What was the purpose of the operation? to repair a retinal detachment or a macular hole. How did the operation go? good, fair or bad. Were there complications? yes or no. What is the prognosis? good or bad. Where was the retinal tear or macular hole? macula, superior-nasal, superior temporal, inferior nasal, inferior-temporal. More specific information may be given by the o'clock coordinates. Therefore, in what position should the patient position his/her head? prone face down, left side down, right side down, other. For how many hours per day? For how many days? What volume and percentage of gas was injected? Should this amount of gas cause complete obstruction of vision, for example the patient sees only a white fog after surgery? For how many days should this last? When will the patient be able to see objects in his upper field of view? Will the patent see strange reflections off the gas-liquid surface? For how long will this last? How many days after the operation should the gas bubble completely disappear? After the surgeon inputs this data, the system can automatically generate a report or a video animation specifically for that patient's operation, explaining exactly what he or she should expect.

5. CONCLUSION

A model is an abstraction of a particular facet of a real system. We developed a model for the absorption of an intraocular perfluoropropane C_3F_8 gas bubble injected during a retinal detachment (RD) operation. We hope that this model can be used to help future RD patients understand the weird visual events accompanying the absorption of an intraocular gas bubble and to help ophthalmologists create brochures and video animations showing their patients what they will see after the operation. Our model has two components: the structural component describes the four geometric configurations that the bubble seems to go through during its lifecycle and the dynamic component describes the rate of absorption of the gas in each of these configurations. A physiological hypothesis that fits this gas behavior is that the rate of absorption of the gas volume is proportional to the amount of gas in direct contact with the retinal surface. Present RD patients do not know what to expect after an operation where a gas bubble is injected into the eyeball. The following is a typical scenario although there is a lot of variability. For a few days after the operation, the patient sees a fuzzy white fog with shadows and bright areas: the surgeon can estimate if this will occur and for how many days it will last. Then the patient starts to see things overhead, like the sky and strange reflections off the gas-liquid surface. The patient's field of view gradually increases over weeks or months, until the gas is all absorbed: the surgeon can estimate how long this will take. A personalized report, given to the patient after the operation, instantiates the details to that particular operation and thus the patient will have some idea of what to expect for the next days, weeks and months.

Funding: This study received no specific financial support.

Competing Interests: The author certify that he has no affiliations with or involvement in any organization or entity with any financial interest (such as honoraria; educational grants; participation in speakers' bureaus; membership, employment, consultancies, stock ownership, or other equity interest; and expert testimony or patent-licensing arrangements), or non-financial interest (such as personal or professional relationships, affiliations, knowledge or beliefs) in the subject matter or materials discussed in this manuscript. The author does not have conflict of interest with the submission; No financial support was received for this submission. This paper has not been presented at a meeting. The authors hereby declare that all experiments have been examined and approved by the appropriate ethics committee and have therefore been performed in accordance with the ethical standards.

Contributors/Acknowledgement: I received no funding for this study. For helpful comments on the manuscript, I thank members of the Systems Engineering Brain Trust: Bruce Gissing, George Dolan and Jerold Swain. I thank Ferenc Szidarovszky for equations. I thank Richard Harding for photographs.

REFERENCES

[1] A. T. Bahill and P. J. Barry, "Multimodal views of the human retina," *Ophthalmology Research: An International Journal*, vol. 2, pp. 121-136, 2014.

[2] A. T. Bahill and P. J. Barry, "A patient's viewpoint of cataract and retinal detachment surgeries," *Ophthalmology Research: An International Journal*, vol. 2, pp. 294-324, 2014.

[3] A. T. Bahill, R. Botta, and J. Daniels, "The Zachman framework populated with baseball models," *Journal of Enterprise Architecture*, vol. 2, pp. 50-68, 2006.

[4] A. T. Bahill and F. Szidarovszky, "Comparison of dynamic system modeling methods," *Systems Engineering*, vol. 12, pp. 183-200, 2009.

[5] M. M. Whitacre, *Principles and applications of intraocular gas*. Boston: Butterworth-Heiinemann, 1998.

[6] M. E. Hammer, *Vitreous substitutes-gas, fluid viscoelastic, silicone, perfluorocarbon, in Duane's Clinical Ophthalmology, eds. Tasman, W.S. and Jaeger, E.A.* Philadelphia: J.B. Lippincott Co, 1994.

[7] G. C. Hartmann, "Physical model for absorption of intraocular gas," *Digital J. Ophthalmology*, vol. 19, pp. 18-20, 2013.

[8] M. Shunmugam, S. Shunmugam, T. H. Williamson, and D. A. Laidlaw, "Air-gas exchange reevaluated: Clinically important results of a computer simulation," *Invest. Ophthalmol. Vis. Sci.*, vol. 52, pp. 8262-8265, 2011.

[9] H. A. Simon, "The architecture of complexity," in *Proceedings of the American Philosophical Society*, 1962, pp. 467-482.

[10] E. W. Weisstein, "Sphere-sphere intersection. From MathWorld--A Wolfram Web Resource." Available http://mathworld.wolfram.com/Sphere-SphereIntersection.html. [Accessed 29 Aug 2014], 2014.

[11] G. F. Hilton and W. S. Grizzard, "Pneumatic retinopexy: A two-step outpatient operation without conjunctival incision," *Ophthalmology*, vol. 93, pp. 626–641, 1986.

[12] J. T. Thompson, "Kinetics of intraocular gases. Disappearance of air, sulfur hexafluoride, and perfluoropropane after pars plana vitrectomy," *Arch Ophthalmol.*, vol. 107, pp. 687-691, 1989.

[13] W. H. Woon, D. Greig, M. D. Savage, D. Spokes, S. Skorski, G. L. Thompson, B. Murphy, and S. Taylor, "Evidence for the aqueous absorption of gas from the eye following vitreoretinal surgery," *Physics in Medicine and Biology*, vol. 53, pp. 3309-3316, 2008.

[14] W. H. Jefferys and J. O. Berger, "Ockham's razor and Bayesian analysis," *American Scientist*, vol. 80, pp. 64-72, 1992.

[15] E. J. Sigler, J. C. Randolph, S. Charles, and J. I. Calzada, "Intravitreal fluorinated gas preference and occurrence of rare ischemic postoperative complications after pars plana vitrectomy: A survey of the American society of retina specialists," *J. Ophthalmology*, vol. 2011, pp. 459 - 463 2012.

[16] S. Bertin and D. Chauvaud, "Simple retinal detachment: Computer reconstruction of visual perception during the first month after surgery," *J Fr Ophtalmology*, vol. 23, pp. 1026-1028, 2000.

[17] M. Goel, R. G. Picciani, R. K. Lee, and S. K. Bhattacharya, "Aqueous humor dynamics: A review," *Open Ophthalmology Journal 1874-3641/10 2010 Bentham Open*, vol. 4, pp. 52-59, 2010.

[18] M. E. Hammer and I. J. Suner, "Leaving on a jet plane: Is any intraocular gas bubble safe for air travel?," *Retinal Physicians*, vol. 7, pp. 58-59, 64, 2010.

[19] A. J. Lockwood and Y. F. Yang, "Nitrous oxide inhalation anaesthesia in the presence of intraocular gas can cause irreversible blindness," *British Dental Journal*, vol. 204, pp. 247-248, 2008.

[20] A. T. Bahill and D. G. Baldwin, "Describing baseball pitch movement with right-hand rules," *Computers in Biology and Medicine*, vol. 37, pp. 1001-1008, 2007.

[21] A. T. Bahill, F. Szidarovszky, R. Botta, and E. D. Smith, "Valid models require defined levels," *International Journal of General Systems*, vol. 37, pp. 533–571, 2008.

[22] E. D. Smith, F. Szidarovszky, W. J. Karnavas, and A. T. Bahill, "Sensitivity analysis, a powerful system validation technique," *Open Cybernetics and Systemics Journal*, vol. 2, pp. 39-56, 2008.

Terry Bahill is an Emeritus Professor of Systems Engineering and of Biomedical Engineering at the University of Arizona in Tucson. He received his Ph.D. in electrical engineering and computer science from the University of California, Berkeley, in 1975. He is the author of six engineering books and over two hundred and fifty papers, over one hundred of them in peer-reviewed scientific journals. Bahill has worked with dozens of high-tech companies presenting seminars on Systems Engineering, working on system development teams and helping them to describe their Systems Engineering processes. He holds a U.S. patent for the Bat Chooser™, a system that computes the Ideal Bat Weight™ for individual baseball and softball batters. He was elected to the Omega Alpha Association, the systems engineering honor society. He received the Sandia National Laboratories Gold President's Quality Award. He is a Fellow of the Institute of Electrical and Electronics Engineers (IEEE), of Raytheon Missile Systems, of the International Council on Systems Engineering (INCOSE) and of the American Association for the Advancement of Science (AAAS). He is the Founding Chair Emeritus of the INCOSE Fellows Committee. His picture is in the Baseball Hall of Fame's exhibition "Baseball as America." You can view this picture at http://sysengr.engr.arizona.edu/.